Two-Dimensional Supramolecular Assemblies of Quinacridone Derivatives: From Achiral to Chiral Racemates and Domains

Zhongcheng Mu, Zhiqiang Wang, and Xi Zhang*

Key Lab of Organic Optoelectronics and Molecular Engineering, Department of Chemistry, Tsinghua University, Beijing 100084, People's Republic of China

Kaiqi Ye and Yue Wang*

Key Lab of Supramolecular Structure and Materials, College of Chemistry, Jilin University, Changchun 130021, People's Republic of China

Received: July 10, 2004; In Final Form: October 5, 2004

We described the two-dimensional (2D) assemblies of *N*,*N*′-dialkyl-substituted quinacridone derivatives on highly orientated pyrolytic graphite (HOPG) observed by scanning tunneling microscopy (STM), and focused on how minor structural variations can influence the supramolecular organization of the compounds. For quinacridone derivatives with or without methyl groups only the same enantiotopic faces of the quinacridone cores are observed with high resolution depending on the length of the substituted alkyl chains. For coadsorptions of quinacridone derivatives and fatty acids at the liquid/graphite interface, we have found interestingly that quinacridone derivatives with methyl groups form chiral racemates, whereas the quinacridone derivative without methyl groups forms chiral domains. The chiral 2D structures formed at the interface are only observed when fatty acids are present as guest molecules and for quinacridone derivatives substituted with long alkyl chains, $-C_{22}H_{45}$. These findings suggest that the 2D nanopatterned structure of quinacridone derivatives with light-emitting properties can be adjusted by controlling intermolecular interaction through tailor-made molecular building blocks and coadsorption.

Introduction

The self-assembly of organic molecules into monolayers on a substrate surface has been extensively studied with scanning tunneling microscopy (STM) in the past decade due to their important roles in many interfacial phenomena and potential applicability to future electronic devices.[1,2] Investigation of the spontaneous separation of an enantiomer or racemate in a two-dimensional (2D) structure has been attracting increasing attention. In the 2D monolayers on achiral solid surfaces, chiral organic molecules separate spontaneously into pure chiral domains,[1,3−6] and achiral molecules also can self-assemble into chiral domains as 2D conglomerates[7−13] or chiral racemates.[14] However, most racemic mixtures and achiral molecules do not spontaneously separate. So far the approaches inducing achiral molecules into chiral domains and racemates include the effects of chain length,[8,14] hydrogen bonding,[12] and solvent effects.[13] To the best of our knowledge, there are few reports on inducing achiral molecules into chiral racemates by means of the coadsorption of two achiral adsorbates.

Quinacridone and its derivatives are well-known as chemically stable pigments and can be used as photovoltaic and photoconductive materials,[15] as well as a dopant in electroluminescent devices.[16] Many investigations on quinacridone derivatives have been devoted to elucidating the effects of structural parameters on the physical properties. For example, Nakahara et al.[17] have synthesized quinacridone derivatives with four alkyl chains and used them in Langmuir−Blodgett films to control the orientation and packing of the chromophores. De Feyter et al.[18−20] have studied the aggregation behavior and two-dimensional ordering of 2,3,9,10-tetra(dodecyloxy)quinacridone, 2,9-di(2-undecyltridecyl-1-oxy)quinacridone, and *N*,*N*′-dimethyl-substituted analogues. Our group has investigated the two-dimensional ordering of *N*,*N*′-dialkyl-substituted quinacridone derivatives with STM[20] and their three-dimensional crystal structures with X-ray diffraction. The steric interaction of methyl groups on the quinacridone core could be used to control stacking interaction between two adjacent chromophores, for improving the performance of electroluminescent devices.

In this work we attempt to investigate the 2D ordering of 1,3,8,10-tetramethyl-*N*,*N*′-dialkyl-substituted quinacridone derivatives, aimed at understanding how steric interaction imposed by the presence of methyl groups on a quinacridone core modulates the orientation of the chromophores at the liquid/solid interface. Moreover, we are wondering whether we can introduce guest molecules to coadsorb with quinacridone derivatives, leading to the formation of 2D chiral racemates or domains from achiral building blocks. The results are believed to be helpful for the design and control of two-dimensional supramolecular assemblies.

Experimental Section

Quinacridone derivatives (Scheme 1) were prepared according to the published method.[18] Stearic acid ($CH_3(CH_2)_{16}COOH$) and palmitic acid ($CH_3(CH_2)_{14}COOH$) were purchased from Sigma-Aldrich and used without further purification. Saturated solutions of quinacridone derivatives and fatty acids in 1-phenyloctane were prepared. A quinacridone derivative solution and fatty acid solution were subsequently mixed in a 1:2 molar ratio. STM

* Corresponding authors.E-mail: xi@mail.tsinghua.edu.cn.

10.1021/jp046942y CCC: $27.50
Published on Web 11/24/2004

SCHEME 1: Chemical Structure of Quinacridone Derivatives

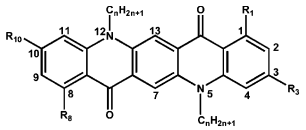

Compound	R_1, R_3, R_8, R_{10}	n
TmQA-C_{16}	-CH_3	16
TmQA-C_{22}	-CH_3	22
QA-C_{22}	H	22

investigations were performed by using a commercial multimode Nanoscope IIIa and Nanoscope (R) IV scanning tunneling microscope (Digital Instrument Co., Santa Barbara, CA) with mechanically cut Pt/Ir (90:10) tips at ambient temperature. All images shown were recorded in the constant-current mode. For measurements at the solution−substrate interface, a saturated solution of a quinacridone derivative or a mixed solution was applied to a freshly cleaved surface of highly orientated pyrolytic graphite (HOPG; Digital Instruments Co.). Measurement conditions are given in the corresponding figure captions. Different tips and samples were used to check for reproducibility and to ensure that there are no image artifacts caused by the tips or samples. Flattening of the images was carried out to compensate for tilting of the substrate and scan line artifacts, and a low-pass filtered transform was employed to remove scanning noise in the STM images.

Results and Discussion

2D Assembly of Pure Quinacridone Derivatives. Before observing coadsorption of quinacridone derivatives and fatty acids, we expected to understand clearly how the pure quinacridone derivatives align at the liquid/solid interface and how the steric interaction of methyl groups affects their 2D assemblies. Figure 1 shows the STM images of TmQA-C_{16} bearing four methyl groups at the 1, 3, 8, and 10 positions of the quinacridone core physisorbed at the liquid/HOPG interface. As may be seen from the large-scale STM image (Figure 1a), TmQA-C_{16} spontaneously forms a stripe pattern on HOPG. The bright part within a stripe may not run through the whole row as marked by blue lines. Figure 1b shows the small-area image of TmQA-C_{16}. The orientation of the molecular cores (green bars) can be clearly seen, while the alkyl chains cannot be resolved. Some rigid cores align in a zigzag way, forming dim areas; others in the same orientation form the bright stripes, as indicated between the two blue lines. These features suggest that the alkyl chains of TmQA-C_{16} are not long enough to resist the influence of the steric hindrance of the methyl groups, thus forming unstable monolayers at the liquid/solid interface.

For TmQA-C_{22} bearing four methyl groups and substituted with substantially longer alkyl chains, we have found that it can form a uniform and stable stripe structure, as shown in Figure 2. A large-area image of the adsorbate structure is shown in Figure 2a. The bright bands correspond to the quinacridone moieties; the dark area corresponds to the alkyl chains. Figure 2b presents a high-resolution STM image in which the direction of the long axis of a quinacridone core is parallel to the boundary of a lamella. The angle between the direction of the long axis of an alkyl chain and the boundary of a lamella is 138.8 ± 2°. Comparing Figure 2b with Figure 1b, we conclude that, when the alkyl chains are long enough, the enhanced interaction between adsorbate and substrate may balance the influence of methyl groups and is responsible for the formation of stable 2D assemblies.

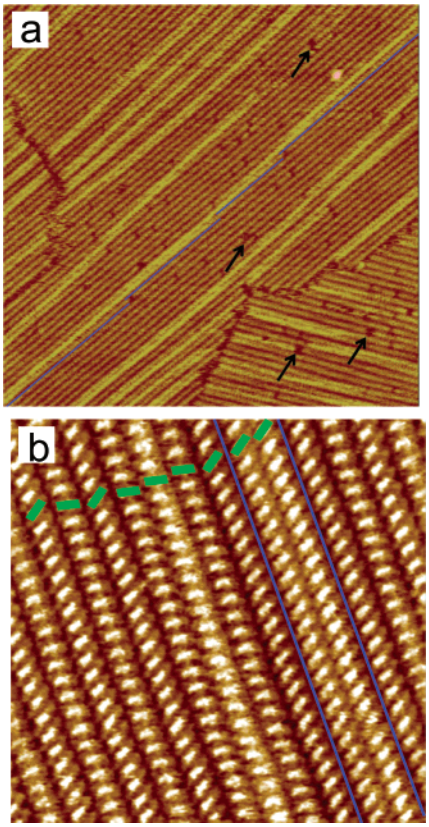

Figure 1. STM images of adlayer of quinacridone derivative TmQA-C_{16} adsorbed on HOPG in phenyloctane. (a) Large-scale image (101.8 nm × 101.8 nm, $U = -1.025$ V, $I = 100.0$ pA). (b) Small-area STM image (23.39 nm × 23.39 nm, $U = -1.000$ V, $I = 50.0$ pA).

To investigate in more detail the influence of the steric hindrance arising from methyl groups on 2D ordering, STM observations on 2D assemblies of QA-C_{22} at the liquid/HOPG interface were carried out. QA-C_{22} differs from TmQA-C_{22} only in lacking methyl groups on its molecular core. As shown in Figure 3, the quinacridone cores are closely packed in bright rows, and two adjacent cores within a row dislocate to some extent along the long-axis direction of a core. For each molecule in the image, the long-axis direction of its alkyl chain is perpendicular to the direction of its core, and the core forms an angle of about 144 ± 3° with respect to the direction of a lamella.

When comparing the 2D structural features of TmQA-C_{22} and QA-C_{22} on HOPG, we realize that the steric interaction of methyl groups can change the pattern structure significantly. For TmQA-C_{22}, molecular arrangement such as the overlap between the adjacent molecular cores within a row in Figure 3 disappears. Because of the presence of methyl groups at the 1 and 8 positions, the interaction between molecules of TmQA-C_{22} became weaker than that between molecules of QA-C_{22}. In addition, the methyl groups at the 3 and 10 positions increase the length of the core, introducing steric hindrance between the adjacent cores within a row. As a result, a completely different motif can be formed by TmQA-C_{22} as compared to QA-C_{22}. Instead, the quinacridone cores align solely along the boundary of the lamella as shown by the stick model in Figure 2b.

2D Assembly of Quinacridone Derivatives with Fatty Acid. We wondered if it would be possible to introduce a guest molecule to modify the adsorbate−adsorbate or adsorbate−substrate interaction in order to induce the formation of chiral racemate. For example, the introduction of fatty acids may modulate intermolecular interactions by interacting with the

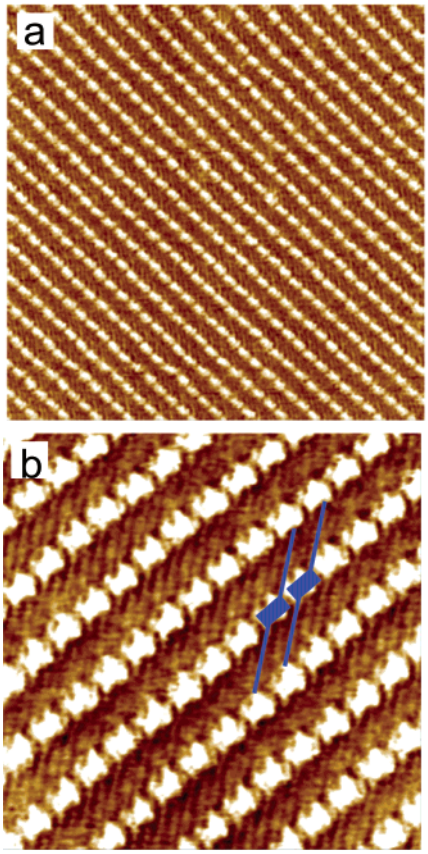

Figure 2. STM images of adlayer of quinacridone derivative TmQA-C_{22} adsorbed on HOPG in phenyloctane. (a) Large-scale image (45.40 nm × 45.40 nm, $U = 800$ mV, $I = 50.0$ pA). (b) High-resolution STM image (20.50 nm × 20.50 nm, $U = -800$ mV, $I = 100.0$ pA).

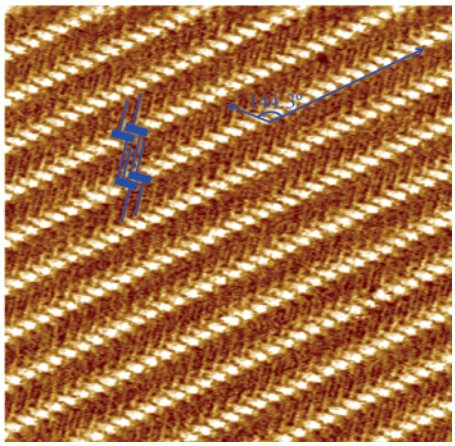

Figure 3. STM image of adlayer of quinacridone derivative QA-C_{22} adsorbed on HOPG in phenyloctane (32.80 nm × 32.80 nm, $U = 850$ mV, $I = 104.3$ pA).

quinacridone host molecules through hydrogen bonding and by enhancing interaction with a substrate, thus probably controlling the structure of 2D supramolecular assemblies on HOPG. Figure 4a is an STM image of the coadsorption of TmQA-C_{22} and palmitic acid on HOPG. The orientation of the quinacridone cores in two adjacent rows points toward different directions, and the angle of a quinacridone core within one row is about 141.29 ± 3° with respect to the direction of the row, while the corresponding angle in the other row is 39.41 ± 3°. The distance (ΔL) between two bright rows was found to be 2.30 ± 0.1 nm, which is larger than the molecular length of palmitic acid and smaller than that of an alkyl chain of TmQA-C_{22}. Meanwhile,

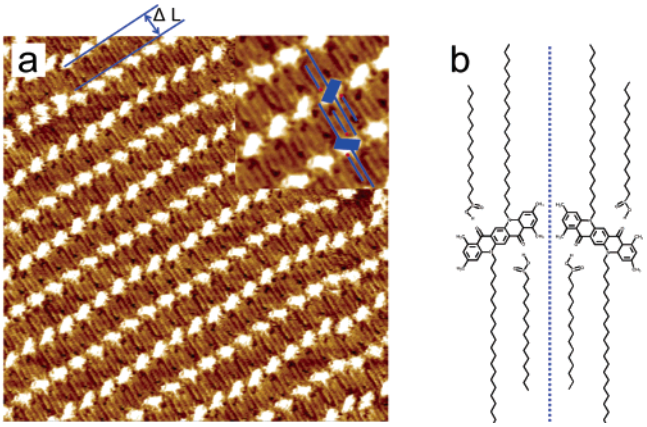

Figure 4. STM image of adlayer of quinacridone derivative TmQA-C_{22} and palmitic acid coadsorbed on HOPG in phenyloctane. (a) High-resolution STM image (33.64 nm × 33.64 nm, $U = 800$ mV, $I = 70.0$ pA). The inset is a magnified image. (b) Schematic chemical structure of two mirror-imaged molecules of TmQA-C_{22}.

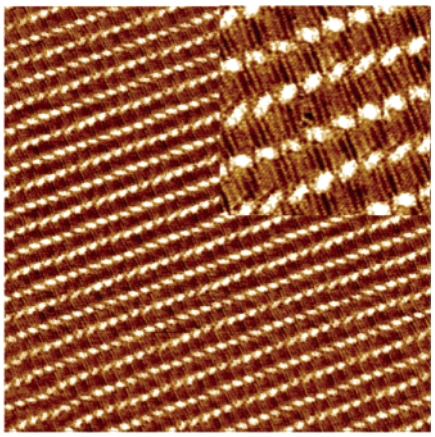

Figure 5. STM image of adlayer of quinacridone derivative TmQA-C_{22} and stearic acid coadsorbed on HOPG in phenyloctane (66.12 nm × 66.12 nm, $U = 800$ mV, $I = 70.0$ pA). The inset is a high-resolution STM image (14.33 nm × 14.33 nm, $U = 800$ mV, $I = 70.0$ pA).

the small holes between the end of an alkyl chain of palmitic acid and a bright row can be seen clearly, indicating that the free volume remains. The arrangements of the alkyl chains from the host and the guest molecules are alternate and interdigitated. The end of an alkyl chain of TmQA-C_{22} also extends into the interspace between two adjacent cores for balancing the free volume. Careful examination of two adjacent structural units belonging to neighboring rows, which are formed by one TmQA-C_{22} and two palmitic acid molecules through hydrogen bonding, reveals that they are mirror images of each other, as shown in Figure 4b. Therefore, we are able to observe the opposite enantiotopic faces of the TmQA-C_{22} molecules in adjacent rows at the same time. When one enantiotopic face of the TmQA-C_{22} molecule is exhibited in a row, the opposite enantiotopic face is exposed in the adjacent one, resulting from the formation of chiral racemate.

If the coadsorption as indicated above can lead to the formation of chiral racemate, it should be also true for the coadsorption of TmQA-C_{22} and other fatty acids with longer alkyl chains, such as stearic acid. As shown in Figure 5, we do obtain an STM image of chiral racemate, which is similar to the 2D structure mentioned above. However, the holes as seen in Figure 4 do not exist in the case of coadsorption of TmQA-C_{22} and stearic acid, which nicely meets our expectation based on the chain-length fitting of the two adsorbates.

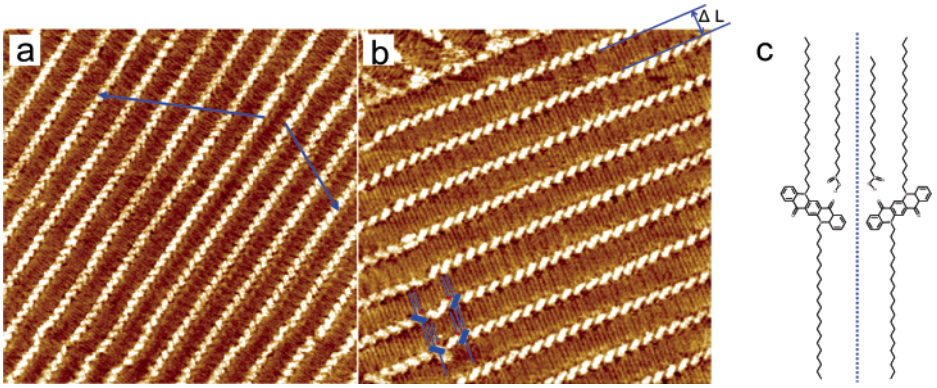

Figure 6. STM images of adlayer of quinacridone derivative QA-C_{22} and stearic acid coadsorbed on HOPG in phenyloctane. (a) Large-scale image (45.58 nm × 45.58 nm, U = 800 mV, I = 60.0 pA) shows two domains with different orientations of quinacridone cores, as indicated in blue arrows. (b) High-resolution STM image (34.17 nm × 34.17 nm, U = 800 mV, I = 50.0 pA). (c) Schematic chemical structure of two mirror-imaged molecules of QA-C_{22}.

As discussed previously, the pure quinacridone derivatives with or without methyl groups can form different 2D structures. We were wondering whether we could have different 2D supramolecular structures for the coadsorption of quinacridone derivatives without methyl groups and stearic acid. In contrast to Figure 5, TmQA-C_{22} is replaced by the hydrogen-bonding acceptor QA-C_{22}. The STM image formed by coadsorption of QA-C_{22} and stearic acid molecules is presented in Figure 6. A large-scale STM image (Figure 6a) shows a uniform stripe pattern, which is separated into two parts in which the long axis of the quinacridone cores points toward different directions, as indicated by arrows. Upon examination of the high-resolution STM image (Figure 6b), it can be seen that each pair of a QA-C_{22} entity and a stearic acid molecule forms a structural unit by means of hydrogen bonding (stoichiometric ratio of 1:1). The structural units aligned in the same long-axis direction as their cores form a domain. In two adjacent domains, both QA-C_{22} molecules and the structural units are mirror images of each other, as indicated by the stick model. Such structures can be regarded as the chiral domains. The distance (ΔL) between two bright rows is 2.57 ± 0.1 nm, which is consistent with the chain length of a $C_{22}H_{45}$ group. The angle between the long-axis direction of a core and the alkyl chain is about 137.79 ± 3°, which is larger than that of pure QA-C_{22} physisorbed at the liquid/HOPG interface, suggesting that the conformation of the QA-C_{22} molecule has changed due to a combination of interactions, including hydrogen bonding, van der Waals interactions, and interaction with the substrate. In contrast to TmQA-C_{22}, the QA-C_{22} molecule has no methyl group at the 1, 3, 8, and 10 positions on its molecular core. Especially the absence of methyl groups at the 3 and 10 positions means that the length of the core is shortened. When coadsorbing with stearic acid at the liquid/HOPG interface, a QA-C_{22} molecule can only combine with one stearic acid molecule to form a structural unit. Comparing the coadsorption of QA-C_{22}/stearic acid and TmQA-C_{22}/stearic acid, we believe that the combined interaction of the steric hindrance introduced by methyl groups and the introduction of guest molecules is responsible for the formation of the chiral racemates in the TmQA-C_{22}/fatty acid system.

In addition, the formation of chiral racemates is dependent on the length of alkyl chains of quinacridone derivatives. Figure 7a, which is the STM image of the coadsorbate of TmQA-C_{16} and palmitic acid, shows clearly that a TmQA-C_{16} molecule and two palmitic acid molecules (1:2) form a structural unit resulting in 2D supramolecular assemblies. The long-axis direction of an individual molecular core is parallel to the

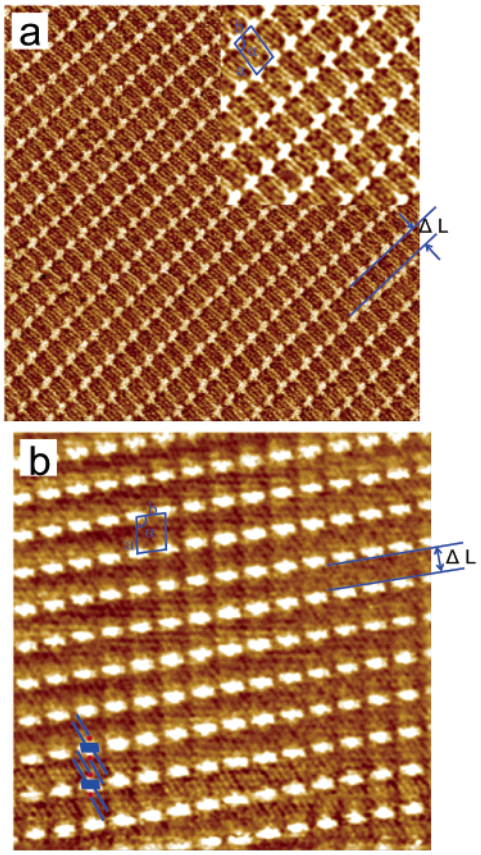

Figure 7. (a) STM images of adlayer of quinacridone derivative TmQA-C_{16} and palmitic acid coadsorbed on HOPG in phenyloctane (43.90 nm × 43.90 nm, U = 800 mV, I = 50.0 pA). The inset is a magnified image. (b) STM image of adlayer of quinacridone derivative TmQA-C_{16} and stearic acid coadsorbed on HOPG in phenyloctane (26.84 nm × 26.84 nm, U = 800 mV, I = 50.0 pA).

boundary of the lamella. The alkyl chains of TmQA-C_{16} are interdigitated, and the two adjacent ones are separated by two chains of palmitic acid molecules which point toward opposite directions. The distance (ΔL) between the adjacent bright rows is about 2.06 ± 0.1 nm, which is consistent with the length of a palmitic acid molecule. Therefore, the acid molecules can extend between the bright rows and form a hydrogen bond with TmQA-C_{16} molecules. The lattice constants of the 2D adlayer were determined to be a = 2.92 ± 0.1 nm, b = 1.72 ± 0.1 nm, and α = 98.3 ± 2°. Figure 7b shows the STM image of the coadsorption of TmQA-C_{16} and stearic acid. It forms a similar

2D structure by coadsorption of TmQA-C_{16} and stearic acid in a stoichiometric ratio of 1:2. The distance ($\Delta L = 1.98 \pm 0.1$ nm) between the adjacent bright rows is almost as large as that of the bright rows formed by TmQA-C_{16} and palmitic acid, although the molecular length of stearic acid is 0.25 nm longer than that of palmitic acid. The unit cell parameters of the 2D assemblies were determined to be $a = 3.04 \pm 0.1$ nm, $b = 2.04 \pm 0.1$ nm, and $\alpha = 96.7 \pm 2°$. Careful examination of the STM image reveals that, in the case of stearic acid, the distance between two neighboring cores within a stripe is obviously larger than in the case of palmitic acid, which may also be confirmed by contrasting the lattice constant of the *b* direction. These findings indicate that the end of the alkyl chain of the stearic acid molecule should be inserted into the interspace between two adjacent cores. The fact that we have never found chiral racemates or chiral domains in the case of coadsorption of either TmQA-C_{16}/stearic acid or TmQA-C_{16}/palmitic acid may suggest that the formation of chiral structures are alkyl chain length dependent.

Conclusions

The two-dimensional assemblies of quinacridone derivatives on highly orientated pyrolytic graphite can be controlled by modifying their chemical structure as well as by coadsorption with fatty acids. We demonstrated that a steric interaction of methyl groups on the quinacridone cores could control the 2D structures formed by quinacridone derivatives. The most interesting finding is the formation of chiral racemates or domains by introducing guest molecules: coadsorption of fatty acids and quinacridone derivatives bearing long alkyl chains and methyl groups gives rise to chiral racemates; coadsorption of fatty acid and quinacridone derivative bearing long alkyl chains but without methyl groups also results in formation of chiral domains. These findings suggest that the 2D patterned structure of quinacridone derivatives with light-emitting properties can be controlled by modifying intermolecular interactions through a combination of tailor-made molecular building blocks and coadsorption.

Acknowledgment. We thank the Major State Basic Research Development Program (Grants G2000078102 and 2002CB6-13401), the Key Project of the Ministry of Education and Natural Science Foundation of China (20334010, 50225313), and the High-Tec 863 Project (2003AA302140) for financial support.

References and Notes

(1) Giancarlo, L. C.; Flynn, G. W. *Acc. Chem. Res.* **2000**, *33*, 491−501.
(2) De Feyter, S.; De Schryver, F. C. *Chem. Soc. Rev.* **2003**, *32*, 139−150.
(3) De Feyter, S.; Grim, P. C. M.; Rücker, M.; Vanoppen, P.; Meiners, C.; Sieffert, M.; Valiyaveettil, S.; Müllen, K.; De Schryver, F. C. *Angew. Chem., Int. Ed.* **1998**, *37*, 1223−1226.
(4) Stevens, F.; Dyer, D. J.; Walba, D. M. *Angew. Chem., Int. Ed. Engl.* **1996**, *35*, 900−901.
(5) De Feyter, S.; Gesquière, A.; Grim, P. C. M.; De Schryver, F. C.; Valiyaveettil, S.; Meiners, C.; Sieffert, M.; Müllen, K. *Langmuir* **1999**, *15*, 2817−2822.
(6) De Feyter, S.; Gesquière, A.; De Schryver, F. C.; Valiyaveettil, S.; Meiners, C.; Sieffert, M.; Müllen, K. *Langmuir* **2000**, *16*, 9887−9894.
(7) Rabe, J. P.; Buchholz, S. *Phys. Rev. Lett.* **1991**, *66*, 2096−2099.
(8) Charra, F.; Cousty, J. *Phys. Rev. Lett.* **1998**, *80*, 1682−1685.
(9) Patrick, D. L.; Cee, V. J.; Morse, M. D.; Beebe T. P. *J. Phys. Chem. B* **1999**, *103*, 8328−8336.
(10) Yablon, D. G.; Giancarlo, L. C.; Flynn, G. W. *J. Phys. Chem. B* **2000**, *104*, 7627−7635.
(11) Böhringer, M.; Schneider, W. D.; Berndt, R. *Angew. Chem., Int. Ed.* **2000**, *39*, 792−795.
(12) Lim, R.; Li, J.; Li, S. F. Y.; Feng, Z.; Valiyaveettil, S. *Langmuir* **2000**, *16*, 7023−7030.
(13) Li, C. J.; Zeng, Q. D.; Wang, C.; Wan, L. J.; Xu, S. L.; Wang, C. R.; Bai, C. L. *J. Phys. Chem. B* **2003**, *107*, 747−750.
(14) Wei, Y. H.; Kannappan, K.; Flynn, G. W.; Zimmt, M. B. *J. Am. Chem. Soc.* **2004**, *126*, 5318−5322.
(15) Hiramoto, M.; Kawase, S.; Yokoyama, M. *Jpn. J. Appl. Phys., Part 2* **1996**, *35*, L349−L351.
(16) Jabbour, G. E.; Kawabe, Y.; Shaheen, S. E.; Wang, J. F.; Morrell, M. M.; Kippelen, B.; Peyghambarian, N. *Appl. Phys. Lett.* **1997**, *71*, 1762−1764.
(17) Nakahara, H.; Kitahara, K.; Nishi, H.; Fukuda, K. *Chem. Lett.* **1992**, 711−714.
(18) Keller, U.; Müllen, K.; De Feyter, S.; De Schryver, F. C. *Adv. Mater.* **1996**, *8*, 490−493.
(19) De Feyter, S.; Gesquière, A.; De Schryver, F. C. *Chem. Mater.* **2002**, *14*, 989−997.
(20) Qiu, D. L.; Ye, K. Q.; Wang, Y.; Zou, B.; Zhang, X.; Lei, S. B.; Wan, L. J. *Langmuir* **2003**, *19*, 678−681.